

Article

Investigation of Vessel Manoeuvring Abilities in Shallow Depths by Applying Neural Networks

Lúcia Moreira *  and C. Guedes Soares 

Centre for Marine Technology and Ocean Engineering (CENTEC), Instituto Superior Técnico, Universidade de Lisboa, 1049-001 Lisbon, Portugal; c.guedes.soares@centec.tecnico.ulisboa.pt
* Correspondence: lucia.moreira@centec.tecnico.ulisboa.pt

Abstract: A set of planar motion mechanism experiments of the Duisburg Test Case Post-Panamax container model executed in a towing tank with shallow depth is applied to train a neural network to analyse the ability of the proposed model to learn the effects of different depth conditions on ship's manoeuvring capabilities. The motivation of the work presented in this paper is to contribute an alternative and effective approach to model non-linear systems through artificial neural networks that address the manoeuvring simulation of ships in shallow water. The system is developed using the Levenberg–Marquardt backpropagation training algorithm and the resilient backpropagation scheme to demonstrate the correlation between the vessel forces and the respective trajectories and velocities. Sensitivity analyses were performed to identify the number of layers necessary for the proposed model to predict the vessel manoeuvring characteristics in two different depths. The outcomes achieved with the proposed system have shown excellent accuracy and ability in predicting ship manoeuvring with varying depths of shallow water.

Keywords: towing tank; planar motion mechanism tests; artificial neural networks; ship's manoeuvring; shallow water



Citation: Moreira, L.; Guedes Soares, C. Investigation of Vessel Manoeuvring Abilities in Shallow Depths by Applying Neural Networks. *J. Mar. Sci. Eng.* **2024**, *12*, 1664. <https://doi.org/10.3390/jmse12091664>

Academic Editor: Md Jahir Rizvi

Received: 14 August 2024

Revised: 9 September 2024

Accepted: 13 September 2024

Published: 17 September 2024



Copyright: © 2024 by the authors. Licensee MDPI, Basel, Switzerland. This article is an open access article distributed under the terms and conditions of the Creative Commons Attribution (CC BY) license (<https://creativecommons.org/licenses/by/4.0/>).

1. Introduction

1.1. State of the Art

In recent years, the tendency toward increasing vessel size has suggested a need to devote attention to the manoeuvring behaviour of ships operating in shallow waters. Because of this scale growth among these ships, the global ease of access to ports is becoming more complicated. To bring down infrastructural and functioning costs for the port's conversion, understanding vessel performance in restricted waters helps in designing practical access. Ship manoeuvrability is greatly influenced by the seabed, ground-bounding waters, and moving vessels. Regarding shallow depths, crucial adjustments on the effect of vessel manoeuvring kinetics have been included in the literature, highlighting that, in restricted conditions, (1) the distance travelled by a vessel's centre of gravity in a course perpendicular to its initial direction when it has altered its course 180° and it is on a reciprocal heading (tactical diameter) may increase mainly because of hull damping effects; (ii) as the vessel resistance increases, the manoeuvring capability decreases, and (iii) the variations in the pressure distribution on the hull can result in greater hydrodynamic forces [1].

Master and deck officers, who ensure the safety of the crew, cargo, passengers, and ship at sea and port, may have complete knowledge on the operation's capabilities in shallow depth and can thus make the right decisions about ship handling. Although manoeuvring data of ships are provided for deep-water conditions, they are usually acquired through full-scale tests or experiments with scaled models. The evaluation of the ship's manoeuvring performance is guided through practical implementation of the Standards for Ship Manoeuvrability (resolution MSC.137(76)) as set by the International Maritime Organization (IMO) [2]. These standards apply to deep-water conditions, and the IMO

recommends that trials be conducted preferably in deep, unrestricted water and that the water distance from the surface to the bottom should surpass the vessel's mean draught by four times. Accordingly, with this recommendation, these trials are unreliable in providing an accurate understanding of vessel manoeuvring in shallow depth because its behaviour differs considerably from when it navigates in high seas. As a result, an accurate prediction of the vessel's manoeuvring operational behaviour in shallow water is essential. The approach formulated and introduced in this paper is built on a neural network system trained with information obtained during a set of planar motion mechanism (PMM) experiments with a ship model executed in a towing tank.

There are numerous studies on and approaches toward vessel manoeuvrability forecasts in different depths; for instance, the steering features of the Esso Osaka were extensively explored by carrying out a series of model test runs and full-scale experiments in the Manoeuvring Committee in the 21st ITTC [3]. It was reported that several effects are increased in shallow depth, such as, the propeller's influence on sway force and yaw moment.

Within the context of the European research project SHOPERA [4], shallow- and deep-water manoeuvring experiments in different sea states have been performed for the KVLCC2 tanker and the Duisburg Test Case (DTC) container ship [5,6]. The benchmark data for manoeuvring in shallow water of DTC ship model were provided at the Fifth International Conference on Ship Manoeuvring in Shallow and Confined Water (MASHCON) for validation and verification [7]. In [8], standard rudder manoeuvre simulations were performed with the KRISO container ship (KCS) travelling at various depths, employing a model based on the Abkowitz formulation. The hydrodynamic coefficients were determined through static and dynamic virtual PMM tests carried out using the Reynolds-averaged Navier–Stokes (RANS) computer program Neptuno created by the authors. The influence of propulsion was represented with a body force model.

The data obtained in the manoeuvring experiments in deep sea entirely fulfil the IMO directions, but for vessels navigating slowly in shallow water, considerably greater distances measured in the tactical circle manoeuvre and significantly lower overshoots and drift angles were found, as expected. PMM test data obtained in a towing tank have been used to evaluate the generalisation performance of numerical models, as in the work presented in [9,10]. A uncertainty analysis of identified hydrodynamic coefficients of a non-linear manoeuvring model is presented in [9]. The dimensionless hydrodynamic coefficients were obtained by employing the least-squares method, truncated singular value decomposition, and Tikhonov regularisation with PMM test data. In [10], the authors present a different version of a least-squares support vector machine (LS-SVM), the truncated LS-SVM, to estimate nondimensionalised hydrodynamic coefficients, also using PMM test data. Recent work using the KCS hull model with a static rudder and a body force model-based propeller is presented in [11] where the respective manoeuvring capabilities are studied and compared in both open and restricted waters.

In [12], the predicting technique of manoeuvring vessel dynamics in shallow depth was explored based on the well-known mathematical manoeuvring group (MMG) model. Through that study, the following conclusions were obtained: The MMG model may be applied for manoeuvring motion prediction in shallow depths; the predicted ship motions agreed fairly well with the observed motions in each water depth; and it is possible to easily predict sinkage and trim in shallow depths using simple forms. In [13], a numerical analysis of vessel dynamics in shallow water was carried out, making use of a commercial unsteady RANS solver. Primarily, the qualities of low-depth waves were examined by performing a set of simulations, and afterwards, a full-scale model of a tanker was employed as a specific instance to forecast its pitch and heave behaviour when subjected to head waves at different depths, embracing a variety of wave frequencies at zero speed. The achieved outcomes have demonstrated that shallow depths have a considerable impact on vertical motions.

Taking into consideration the differences between inland and open seas, a particular system of manoeuvrability assessment methods for inland vessels, which has been

suggested to differ in testing manoeuvres and standards, appears eligible [14]. The assessment of the manoeuvring operational behaviour of a vessel has been treated using approaches that imply solving simplified mathematical models or obtaining the complete set of hydrodynamic coefficients from tests, computational fluid dynamics (CFD), or potential theory [15–17]. The reliability of simplified formulations greatly depends on the effectiveness of hydrodynamic coefficients, experimental data are very expensive, and it is challenging to equip a ship model and arrange the facilities required for this purpose. Also, obtaining hydrodynamic coefficients through CFDs is computationally costly.

This work's motivation is to report an alternative and effective approach for modelling non-linear systems through artificial neural networks (ANNs) that address the manoeuvring simulation of ships and, in this specific case, in shallow water. Neural networks have been employed to simulate manoeuvring behaviour [18]. The development of the processing capability of computers allows the execution of complex algorithms into advanced decision support systems in maritime navigation [19]. These systems should incorporate functions such as providing solutions for ship manoeuvring operations and navigational situations.

These demands may be achieved through neuroevolutionary methods with ANNs. ANN is so called because the model imitates the learning mechanism of the human brain and does not rely on a physical representation. As a result, it is more effective than traditional physics-based models, particularly when they are complex. The neural network (NN) approach reported here has been demonstrated to be an interesting option for substituting mathematical models for ship manoeuvring that are based on physics. The necessary information for training this NN-based model might be directly acquired from full-scale sea trials or free-running model tests so that the technique is sufficiently precise for acquiring complete experimental information. This type of model also has the advantage of being fast, with a computational time for each training run varying between 9 and 36 s for the presented case, using a 13th Gen Intel(R) Core(TM) i7-1355U (1.70 GHz) processor.

In [20], the authors applied ANNs to represent the manoeuvring characteristics of a chemical tanker based on test results acquired with a model. In their studies, the ANNs were used to estimate the yaw angle and the paths followed by the model resulting from the rudder angle order, the number complete rotations by the propeller shaft, the x and y positions, sway velocity, and yaw angle values measured at the preceding instant. The data obtained from the learning procedure using the Levenberg–Marquardt technique were analysed and contrasted with the results obtained using the scaled conjugate gradient method and the Bayesian regularisation process. In [21], the authors studied an approach that employs a genetic algorithm to optimise the weights and the number of backpropagation neurons of an NN at the same time to estimate the path of the vessel. Other applications of neural networks for ship manoeuvring were presented in [22–26].

More recent applications in the navigation field have focussed on vessel-added resistance prediction in waves to verify its fitness with both the practical and technical standards recommended by the IMO for mitigating emissions of air pollutants from vessels [27]. The research presented in [28] shows the development of a mathematical approach established on the results of fluid dynamics computation in head waves and machine learning, specifically ANNs. The model has demonstrated that it can accurately calculate the added resistance of container vessels based on vessel particulars, travelling speed, and sea state by using two wave energy spectra. Then, in [29], an ANN was employed to estimate the added resistance coefficient for container vessels in regular head waves of diverse speeds. The information meant to train the model was derived from computational analysis by applying the Boundary Integral Element Method considering several container vessels' hull forms. In [30], the predictive ability of recurrent neural networks (RNNs) was explored for real-time short-term prediction (nowcasting) of vessel motions in high seas. RNN capabilities, long short-term memory (LSTM), and gated recurrent unit (GRU) approaches were evaluated and compared through a data record derived from CFD simulations of a self-propelled destroyer ship navigating stern-quartering waves in sea state seven. Gener-

ally, all the procedures provided good and similar results. In [31], to set up data-driven recurrent mapping within ship motion dynamics, an ultrashort-term deep learning predictor was developed, establishing a self-attention-weighted bidirectional long short-term memory (Bi-LSTM) network together with one-dimensional convolution (Conv-1D). The Bi-LSTM has been used to learn forward and reverse feature maps of ship manoeuvring time-series data. At the same time, the self-attention mechanism, cascaded in the serial mode, is contrasted with traditional techniques such as dynamic mode decomposition (DMD), support vector regression (SVR), GRU, and LSTM models. In [32], to facilitate ship manoeuvring fast-dynamics prediction, which is imperative within motion planning and control, a self-organising data-driven network with hierarchical pruning (SDN-HP) is introduced using a fuzzy neural architecture.

In [33], a procedure is developed with LSTM NNs to represent the motions of a free-running David Taylor Model Basin (DTMB) 5415 destroyer operating at 20 knots in sea state 7 stern-quartering long-crested irregular seas. The presented work has shown that LSTM NNs can be trained to accurately represent the six-degree-of-freedom response of a free-running vessel in waves. A rigorous and comprehensive case study demonstrated the methodology's effectiveness for accurately representing the non-trivial motions of the considered hull form. In [34], a new hybrid prediction model of ship motion attitude is suggested based on LSTM NNs and Gaussian process regression (GPR). The results obtained with the presented method have shown that the LSTM-GPR hybrid predictor effectively integrates the advantages of the high prediction accuracy of the LSTM model and the interval prediction potential of the GPR model and successfully verified the effectiveness and advancement of the LSTM-GPR hybrid model.

The research presented in [35] focusses on a model-free machine learning method for 'ship0as a wave buoy' (SAWB)-based sea state estimation (SSE), using NNs to map vessel response spectral data to statistical wave properties for a small uninhabited surface vessel. The ANN models trained using heave, pitch, and roll vessel response data have been shown to be able to estimate significant wave heights, mean wave periods, and relative wave headings effectively for idealised sea states within the given constraints. The main goal of the work presented in [36] was to develop a seakeeping prediction tool to be used in the early stages of ship design. Therefore, an artificial intelligence (AI) algorithm based on ANNs was developed, and it only required a number of ship coefficients of form. The data were generated using a frequency-domain seakeeping code based on the boundary element method (BEM). The work has shown the capability of ANNs to compute seakeeping loads quickly, achieving more than 200 ships per second. Furthermore, the ANNs can naturally remove irregular output data computed by BEM solvers.

In [37], the novel attention-based neural network (AT-NN) was applied to estimate wave height, zero-crossing period, and relative wave direction from raw time-series ship pitch, heave, and roll data. Despite reduced input data, it was demonstrated that the suggested methods by adjusted state-of-the-art approaches (based on convolutional neural networks (CNNs) for regression, multivariate LSTM CNN, and sliding puzzle NN improved estimations of the mean-squared error (MSE), the mean absolute error (MAE), and Nash–Sutcliffe efficiency (NSE) by up to 86%, 66%, and 56%, respectively, compared to the best-performing original methods for all sea state parameters. Moreover, the presented method based on AT-NN outperformed all the tested procedures (original and enhanced), improving estimation MSE by 94%, MAE by 74%, and NSE by 80% when examining all sea state parameters. In [38], a hybrid spatial–temporal NN that integrates a CNN and a multi-recurrent neural network (MRNN) is presented. The spatial and temporal features were extracted from a time series using a CNN and an MRNN, respectively. Afterwards, the spatial features were input into the MRNN and used as auxiliary features to predict ship motion. To determine the most suitable hyperparameters, the authors introduced an improved adaptive particle swarm optimisation (IADPSO) algorithm that includes a novel population initialisation procedure and dynamic adaptive parameter tuning to optimise the algorithm's global- and local-search capabilities. An actual ship's pitch, roll, and heave

motion data were used to assess the IADPSO–CNN–MRNN hybrid prediction model. The results showed that the presented prediction model fitted the actual data better in regions with significant variations. Moreover, it surpassed the CNN–LSTM, CNN–GRU, LSTM, and GRU models regarding prediction performance.

The literature referred to above on the NN approach mainly addresses ships' wave-induced motions. The present paper addresses manoeuvring models in which the motion is on the horizontal plane, which means that there are no effects of waves. Therefore, the use of ANNs in ship manoeuvring applications appears promising and exhibits a good level of reliability. An alternative system identification procedure for creating a low-speed manoeuvring model making use of RNNs and free-running model tests is suggested in [39]. The authors mainly examined a low-speed manoeuvre, like the final stage in berthing, to attain automatic berthing control. Also, a new loss function that attenuates the impact of the noise included in the training data is presented. Recent work focussed on a mathematical model of the cooperative manoeuvres of autonomous ships, autonomous tugboats, or remotely controlled tugboats that are expected to be an essential part of navigation assistance for safe navigation in ports and for berthing/unberthing operations is presented in [40]. The authors presented a new mathematical model framework for cooperative manoeuvres that considers the coupled motions among tugboats and a ship as precisely as possible.

Given the advantages of the NN approach, it is assumed that the results achieved by ANN simulations can accurately reproduce the natural features of a vessel manoeuvring in shallow depth. Until now, research related to ships' manoeuvrability simulations applying ANNs has predominantly focussed on their evaluation in deep waters, as mentioned before.

Particularly, an analysis focussed on studying ship manoeuvrability in shallow depths, which has been shown to be restricted in quantity and extension. An optimal truncated LS-SVM for calculating non-linear manoeuvring models' dimensionless coefficients in shallow water was presented in [41]. In [42], the authors used the method referred to before with a Quantum-inspired evolutionary algorithm (QEA) to perform manoeuvring simulations of a container ship in low water depth, taking into account the water depth influence, only examining manoeuvrability of a ship type in two shallow-depth conditions. Considering the absence of prior investigations regarding vessel manoeuvrability simulations in shallow depth through NNs, the analysis described in the present study was conducted to assess an ANN's ability to learn the influence of distinct shallow depths on a vessel's manoeuvring characteristics.

1.2. Aim of This Work

This paper analyses the manoeuvring behaviour of the DTC ship in various shallow depths. A set of PMM experiments, namely, pure drift, pure sway, pure yaw, and mixed yaw and drift, were conducted with the model of the DTC ship in the towing tank of Flanders Hydraulics Research (FHR) [43]. Different sets of inputs are used for training an NN to estimate different outputs:

- (1) Surge and sway velocities, yaw rate, x and y positions, course, and depth are input to estimate the surge force, sway force and yaw moment;
- (2) Surge and sway forces, in addition to the yaw moment, positions x and y , course, and depth, are input to estimate surge and sway velocities and yaw rate.

In the current paper, the network is trained using the Levenberg–Marquardt algorithm, instead of the backpropagation method employed before in other previous applications of ANNs to the manoeuvring prediction problem [16,44,45]. This procedure is employed to solve non-linear least-squares problems, and it is a combination of two other methods: gradient descent and Gauss–Newton algorithms. As there are two possibilities for the algorithm's direction at each iteration, the Levenberg–Marquardt algorithm is more robust than the Gauss–Newton algorithm. As an advantage, it shows to be faster at converging than either the Gauss–Newton or gradient descent algorithm. Furthermore, it can handle

models with multiple free parameters that are not precisely known. The algorithm can still find an optimal solution if the initial guess is far from the mark.

This paper is organised in the following terms: the next section explains the PMM tests performed in shallow water with the DTC model; Section 3 introduces the NN assumed in this paper and describes the learning method; Section 4 analyses the proposed model effectiveness; and then, in the last section, our final remarks are stated.

2. Planar Motion Mechanism Experiments in Shallow Water

The PMM experiments with a vessel model and the data used to train the ANN in this work are presented below. The experiments were executed by Flanders Hydraulics Research (FHR) as part of the SHOPERA project [6,46]. Overall, 102 PMM experiments (pure sway, pure drift, and pure yaw) were conducted considering distinct depths, velocities, amplitudes, and sample periods, as might be observed below in Table 1.

Table 1. PMM matrix tests executed by FHR [42].

Class	h^a	V^b	β^c	A^d	T^e	n^f
Pure Sway	2	3	7	1	4	12
Pure Drift	2	3	7	-	-	28
Pure Yaw	2	3	7	3	2	62

^a Depth (m): 0.3254, 0.1952. ^b Full-scale velocity (kn): 6, 11, 16. ^c Drift angle (°): 0, ±2.5, ±5, ±10. ^d Oscillation motion amplitude: Pure sway (m): 0.2; Pure yaw (°): 5, 10, 15. ^e Period (s): Pure sway: 20, 40, 60, 80; Pure yaw: 17, 25. ^f PMM tests' overall value: 102.

A Post-Panamax-container scaled model was employed throughout the tests. This container model (the DTC vessel) [43,47] is widely used, and the principal information about its characteristics is specified in Table 2. The DTC is a conventional 14,000 TEU container ship hull structure made at the Institute of Ship Technology, Ocean Engineering and Transport Systems, to measure and verify computational techniques [43]. The DTC is a single-screw ship with a bulbous bow, a big bow flare, a great stern overhang, and a transom stern. The vessel was experimented on with a bare hull and a hull with appendages prepared with a fixed-pitch propeller with five blades and clockwise rotation and a twisted rudder with a Costa bulb. The container model was built at a 1:89.11 scale.

Table 2. Model specifications [47].

Parameter	Units	Value
λ	1	1:89.11
L_{PP}	m	3.984
B	m	0.572
T_{design}	m	0.163
∇	m ³	0.2458
C_B	1	0.661
S	m ²	2.777
L_{CB} from AP	m	1.953
\overline{KG}	m	0.222
\overline{GM}	m	0.058
I_{xx}	kg.m ²	13.7
I_{yy}	kg.m ²	211.6
I_{zz}	kg.m ²	219.2

Until the present time, the best procedure for gathering the information needed for simulating manoeuvres when a ship is subject to quite exceptional circumstances, like port manoeuvres at low speed in shallow depth and restricted water, seems to be the conduction of captive manoeuvring experiments either in a towing tank or in a circulating water channel [48–50]. Additionally, the towing tank qualities establish the experimental

arrangement of the model. In the case of the FHR towing tank, the dimensions (see Table 3) enable the use of vessel models with a dimension of generally 4 m in length. The towing tank specifications and potential have been broadly reported in [51]. In captive mode, it is possible to place the model of the vessel in the three horizontal degrees of freedom (surge, sway, and yaw) with roll free or fixed and with pitch and heave remaining free all the time. The roll was fixed throughout the experiments. The captive setup is presented in Figure 1. Throughout captive tests, the ship is fixed in the horizontal plane (surge, sway, and yaw), enabling roll, pitch, and heave (during the calm water tests, the roll is fixed, and then, the moment is measured). The hull forces are measured using load cells LC1 (separate measurements of X and Y forces) and LC2. The ship’s heave, trim, and roll are measured by using four potentiometers, P1 to P4 (see Figure 1).

Table 3. FHR towing tank’s basic dimensions [47].

Dimension	Units	Value
l_{Total}	m	87.5
$l_{Effective}$	m	68.0
b	m	7.0
h (max.)	m	0.5
$L_{Vessel Models}$	m	3.5 till 4.5

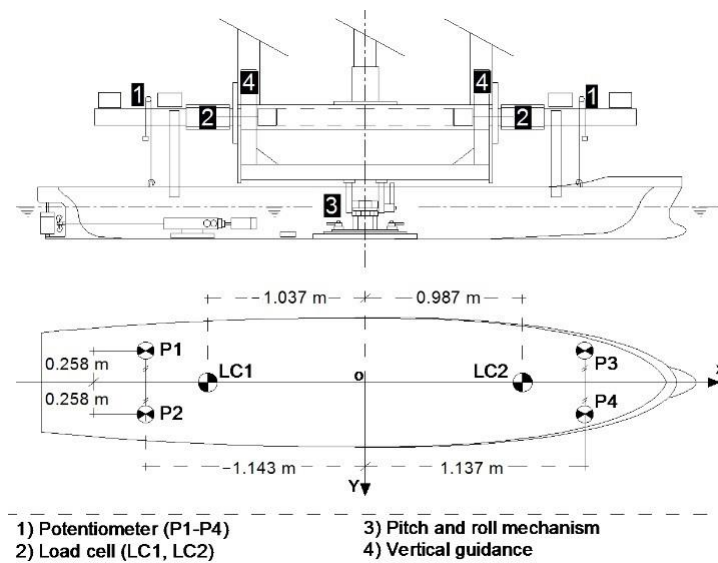


Figure 1. Setup for captive tests.

Figure 2 shows three rectangular and clockwise reference frames. $O_0x_0y_0z_0$ is the earth-bound towing tank frame of reference. The vertical O_0z_0 -axis points downwards, whereas the horizontal O_0x_0 - and O_0y_0 -axes are positioned at the free surface of the water at rest. $O_0x_0z_0$ is the towing tank’s longitudinal vertical symmetry plane.

The reference information comprises harmonic yaw and sway experimental data obtained with the DTC bare hull. The vessel model performed pure sway motions for a given sway amplitude and testing period throughout the harmonic sway experiment. During the harmonic yaw experiment, the vessel model performed pure yaw motions under a selected yaw amplitude and testing period. The vessel model maintained a null drift angle throughout the harmonic yaw experiments. The longitudinal element u was maintained at a fixed value throughout the two experiments. The experiments have also been performed with the hull with appendages at null propeller rotation speed and the model self-propulsion point. Different groups of experiments, for example, stationary experiments at a fixed speed with or without drift and without yaw, were included as a

source to demonstrate the correlation between the kind of experiment and the kinematical testing parameters.

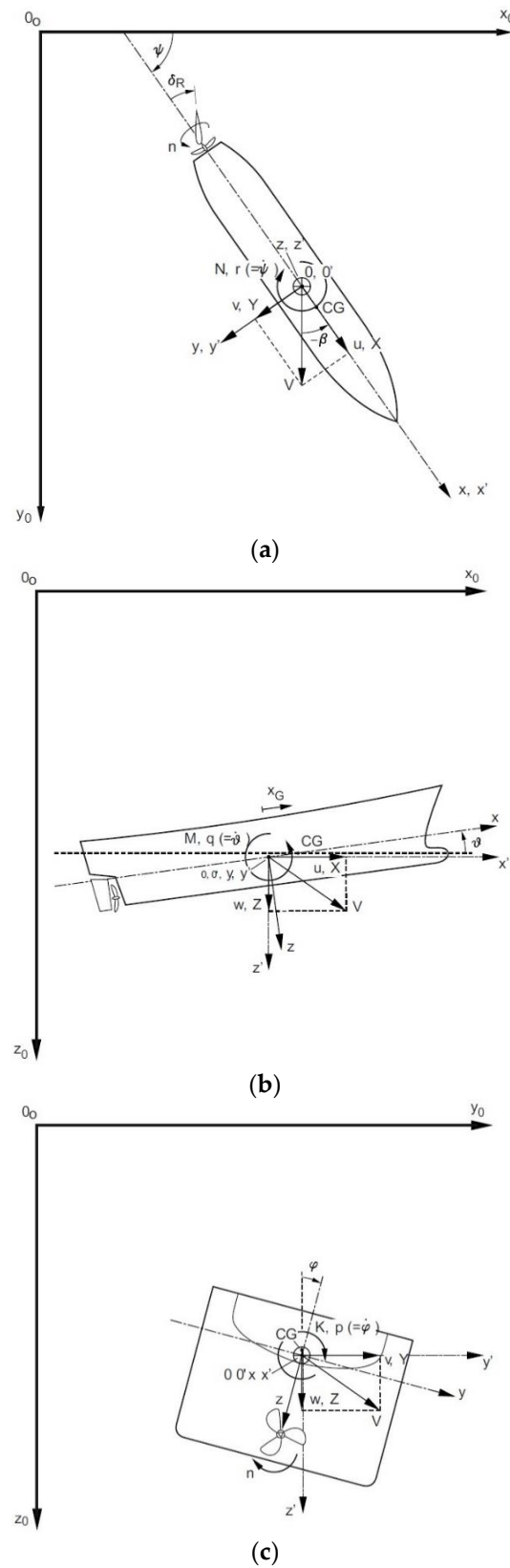


Figure 2. Vessel- and earth-bound (towing tank) reference frame projections: (a) on the $O_0x_0y_0$ plane; (b) on the $O_0x_0z_0$ plane; (c) on the $O_0y_0z_0$ plane.

3. Artificial Neural Network (ANN)

3.1. Model

NNs are computational models that mimic the complex functions of the human brain. NNs are mainly separated linkages of adaptive random processing elements (PEs); meaning that a connected group of mathematical functions forms these elements, and the information is converted by applying a probabilistic viewpoint for computation. Nevertheless, implemented in data processing devices, a PE is generally a simple unit that receives several input signals and, based on those inputs, either generates a single output signal or does not (McCulloch–Pitts model). The numeric values related to the links between neurons (synapses), called weights, are the variables corrected throughout the learning process to minimise the discrepancy between the current and target outputs.

The NN system works over interrelated layers, transforming input information into significant models. The input layer acquires the primary data, which is subsequently entered within at least one hidden layer that executes numerical computations. The output layer generates the outcomes, like estimations or classifications. Adaptation refers to the ability of the network to modify its structure or connection weights in response to feedback signals from the environment. Adaptive NNs are characterised by online learning, which allows them to learn from new data as they become available. An NN is an arbitrary mathematical statistical modelling implementation. They can find and represent non-linear and complex input–output relationships; produce generalisations and inferences, reveal hidden relationships, patterns, and predictions; and model extremely volatile information and deviations required to forecast infrequent occurrences.

MLPs are the dominant NN topology in use. Lippmann [52] reported among the predominant literature about MLPs' mathematical abilities. Usually, for steady pattern categorisation, the two hidden layers of an MLP are a standard pattern classifier. Namely, the discriminant analysis may assume any configuration required by the input information collection. Finally, while the output and the weight sets are properly normalised, the MLP achieves the highest analytical recipient performance, which is great in terms of a classifying perspective [53]. Concerning mapping effectiveness, the MLP is equivocally able to approximate stochastic processes.

MLPs are commonly trained by applying the backpropagation process, and in this work, the Levenberg–Marquardt algorithm solves the minimisation problem. The bias and weights are adjusted to ensure minimisation, and the backpropagation technique is used for the Jacobian matrix calculation of the performance function concerning the bias and weights.

Indeed, backpropagation capabilities have partially driven increased interest toward NNs. Least mean squares (LMS) cannot be implemented for hidden PEs since the target signal is not known in that training approach. The backpropagation learning method disseminates errors through the structure and allows the adaptation of the hidden PEs.

Two of the principal characteristics of MLPs are their arbitrary PEs, which own a threshold which is supposed to be smooth (the hyperbolic tangent function and the sigmoid curve are dominant and globally chosen), and their inherent large linkage (basically, an element that lies in a certain layer feeds each element of the subsequent layer). MLPs are trained through the supervised error-correction learning rule, which implies that the network-target output needs to be reached. In pattern recognition, this is the usual practice because the input information has specifications (that is, which data belong to which test is found out). A common arrangement illustration of a singular-hidden-layer MLP configuration is shown in Figure 3.

A singular bias neuron b is added to all the inputs p_j and hidden layers, which are summed to the weighted inputs w_j for the calculation of the network input n , which is denoted through

$$n = \sum_{j=1}^n w_j p_j + b \quad (1)$$

The number of hidden neurons controls the network architecture’s robustness. This amount is carefully chosen through a sensitivity analysis of the findings after the execution of various training runs for certification.

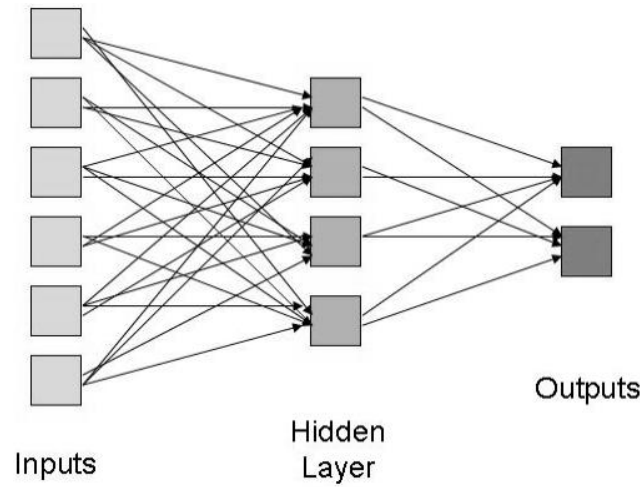


Figure 3. A general elementary feed-forward network representation.

In this work, two distinct configurations of MLP networks (feed-forward NN) are implemented using MatLab R2024a, trained with the Levenberg–Marquardt procedure, and contrasted with the resilient backpropagation method afterwards. The primary MLP is composed using a node set organised in three layers: an input layer, a hidden layer, and an output layer; the other MLP contains an input layer, three hidden layers, and an output layer. Except for the input nodes, all the nodes are neurons that use a non-linear activation function, which, in this present instance, is a sigmoid curve. For this study, the training procedure is executed for two distinct learning cases using seven input and three output nodes, as shown in Table 4 (I is the input, and O is the output). The results are compared using an MLP configuration with one and three hidden layers. A composition of ten hidden neurons is selected in the additional analysis of the method convergence and generalisation ability regarding the instance of the MLP with one hidden layer, and a combination of [5,8,10] neurons is chosen for the case of the MLP with three hidden layers. The training is carried out using the Levenberg–Marquardt technique, and then, the performance is contrasted with the one achieved by training the network with the resilient backpropagation approach. The adopted input–output variables are as follows:

- h —depth;
- x —longitudinal position of the ship;
- y —transversal position of the ship;
- COG —course over ground;
- u —surge velocity;
- v —sway velocity;
- r —yaw velocity;
- X —surge force along the x -axis;
- Y —sway force in direction of the y -axis;
- N —moment about the z -axis.

Table 4. Matrix of the training tests.

#	Set									
	h	x	y	COG^c	u	v	r	X	Y	N
1	I	I	I	I	I-	I-	I	O	O	O
2	I	I	I	I	O	O	O	I	I	I

3.2. Training

The sigmoid transfer functions commonly employed by the multilayer networks in the hidden layers are known under the “squashing” functions since those functions press an unlimited input domain in a limited range of outputs. These types of functions can be identified because their gradients approximate zero when the input becomes larger. So, an issue is generated once the steepest descent is applied for the multilayer net training with sigmoid functions because the slope may be very small and, thus, generate slight variations in the biases and weights despite the fact that they are not optimum results.

The resilient backpropagation optimisation objective is to annul the undesirable impacts of the partial derivative quantities. The derivative sign may provide the direction of the weight update; the derivative magnitude does not affect the weight update. The weight alteration magnitude depends on a distinct update value. The update value for all the biases and weights is augmented by a factor any time the performance function derivative in respect of that weight obtains identical signs in two consecutive iterations. The updated value decreases by a factor anytime the derivative, with respect to that weight, modifies the sign over the preceding iteration. As long as the derivative is null, the update value does not change. Anytime the weight fluctuates, its modification decreases. The weight variation amplitude rises as long as the weight changes continuously along a constant direction for multiple iterations. A detailed explanation of resilient backpropagation optimisation is presented in [54]. This method is meant to contrast with the results acquired using the Levenberg–Marquardt algorithm.

Inputs and outputs were connected in a single hidden layer with ten neurons. A sigmoid is used as an activation function and takes effect in all the neurons in the hidden layer, generating a system that ensures smooth results. The activation function is stated by the following:

$$f(x_i) = \frac{e^{x_i}}{e^{x_i} + 1} \quad (2)$$

where x is the input of neuron i .

The data obtained in the PMM tests are put into array form and then split according to the percentages below:

For training, 80% of the data points are used;

For validation, 10% of the data points are used;

For testing, 10% of the data points are used.

The total number of data points used for the training procedure was 23,475, corresponding to 18,780 for the training set, 2315 for the validation set, and 2314 for the testing set.

Generally, MLP training is conducted using the backpropagation algorithm; however, in the present case, the damped least-squares algorithm, alternatively called the Levenberg–Marquardt method, is used, as well as the resilient backpropagation algorithm method for comparison.

The error-correction learning executes in the following way: from the network output at PE i at iteration n , $y_i(n)$, and the desired output $d_i(n)$ for a specified input instance, an instantaneous error $e_i(n)$ may be created using

$$e_i(n) = d_i(n) - y_i(n) \quad (3)$$

Backpropagation determines the cost function sensitivity regarding all the network weights and renews them according to the sensitivity [55]. Its advantage is that it can be employed in local data, and only some products per weight are needed, which is highly efficient. Its handicap is that as the procedure is a gradient descent approach, it only uses local data and can consequently become stuck in relative minima. Moreover, the procedure is naturally noisy since a poor gradient approximation is assumed, generating a slow convergence problem.

Despite the fact that backpropagation is a gradient descent method, the Levenberg–Marquardt algorithm is based on Newton’s method, which is outlined to minimise functions which are summations of non-linear-function squares [56], as the following configuration:

$$E = \frac{1}{2} \sum k(e_k)^2 = \frac{1}{2} \|e\|^2 \tag{4}$$

where e_k is the error in the k -th exemplar and e is the vector of the elements e_k . Since the divergence among the previous and actual weight vectors is insignificant, the error vector might be approximated to a tangent line applying the Taylor series:

$$e(j + 1) = e(j) + \frac{\partial e_k}{\partial w_i} (w(j + 1) - w(j)) \tag{5}$$

Thus, the error function might appear in the following form:

$$E = \frac{1}{2} \left\| e(j) + \frac{\partial e_k}{\partial w_i} (w(j + 1) - w(j)) \right\|^2 \tag{6}$$

Keeping the error function to a minimum in respect of the actual weight vector:

$$w(j + 1) = w(j) - (J^T J)^{-1} J^T e(j) \tag{7}$$

with $(J)_{ki} = \frac{\partial e_k}{\partial w_i}$ representing the Jacobian matrix.

The Hessian matrix for the sum-of-squared-error function is denoted by the following:

$$(H)_{ij} = \frac{\partial^2 E}{\partial w_i \partial w_j} = \sum \left\{ \left(\frac{\partial e_k}{\partial w_i} \right) \left(\frac{\partial e_k}{\partial w_j} \right) + e_k \frac{\partial^2 e_k}{\partial w_i \partial w_j} \right\} \tag{8}$$

Omitting the second term in (8), the matrix may be updated in the following form:

$$H = J^T J \tag{9}$$

The weight change has to obtain the Hessian inverse. The matrix is quite simple to calculate as it has a basis on first-order partial derivatives with respect to the network weights, which are easy to manage via the learning process. Even though the updating equation is applied recursively to lower the error function, the procedure can create a big step size, which may invalidate the first-order approximation that has established the equation. With the Levenberg–Marquardt method, the error function is minimised, whereas the step size is low, which guarantees an effective first-order approximation. This minimisation is captured using a modified error function, defined as follows:

$$E = \frac{1}{2} \left\| e(j) + \frac{\partial e_k}{\partial w_i} (w(j + 1) - w(j)) \right\|^2 + \lambda \|w(j + 1) - w(j)\|^2 \tag{10}$$

with λ being a parameter that controls the step size. The modified error is minimised in respect to $w(j + 1)$:

$$w(j + 1) = w(j) - (J^T J + \lambda I)^{-1} J^T e(j) \tag{11}$$

Once λ is zero, Equation (11) just outlines Newton’s method, applying the approximation to the Hessian matrix. When λ is high, the method changes to the steepest descent with a small step size. Newton’s method is more expedited and precise once it is about an error minimum; therefore, the goal is to turn to Newton’s method expeditiously. Thus, λ is decreased following each effective step (decrease in performance function) and rises only if a certain step leads to a performance function augmentation. Consequently, the performance function reduces with each step during the iterative process.

A representation of the proposed feed-forward NN is presented in Figure 4.

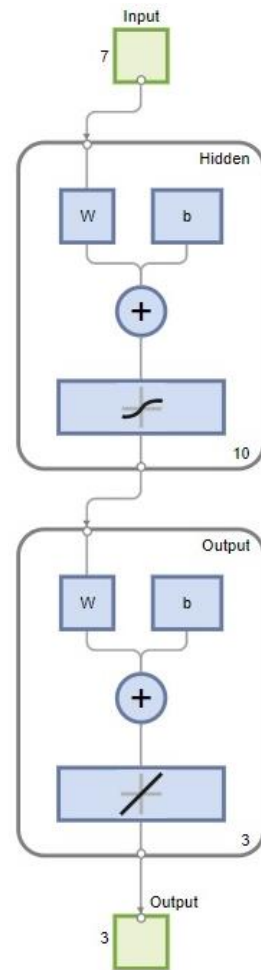


Figure 4. Picture of the network outline.

4. Results

Figures 5–7 show the predicted and experimental longitudinal and transversal forces X , Y , and the yaw moment N , respectively, for different water depths, using the Levenberg–Marquardt method with one hidden layer in the network structure. Figures 8–10 present boxplots of the errors obtained in the predictions shown in Figures 5–7, respectively. The boxplots allow for a clear summary of the error data, displaying the median, upper quartile, lower quartile, minimum, and maximum values. The outliers can also be easily seen.

In Figures 5–7, the ANN system can visibly reproduce the forces and moments obtained throughout the PMM test with great precision. It can also be seen that the variation in the shallow water was learned by the NN model. From the boxplot of Figure 8, which compares the central tendencies of the X force for the two different depths, it can be verified that the median is slightly similar. The variability for $h = 0.1952$ m is slightly higher, but this is due to the forces measured for this depth also being slightly higher than that for $h = 0.3254$ m. It perceived that for both depths, the distribution of the obtained error is right-skewed. Similar results are obtained for the boxplot of the Y force presented in Figure 9. The boxplot of the N moment shown in Figure 10 shows a difference in the distribution of the error for the different depths. For the case of $h = 0.3254$ m, there is a symmetrical distribution; for $h = 0.1952$ m, the error presents a right-skewed distribution.

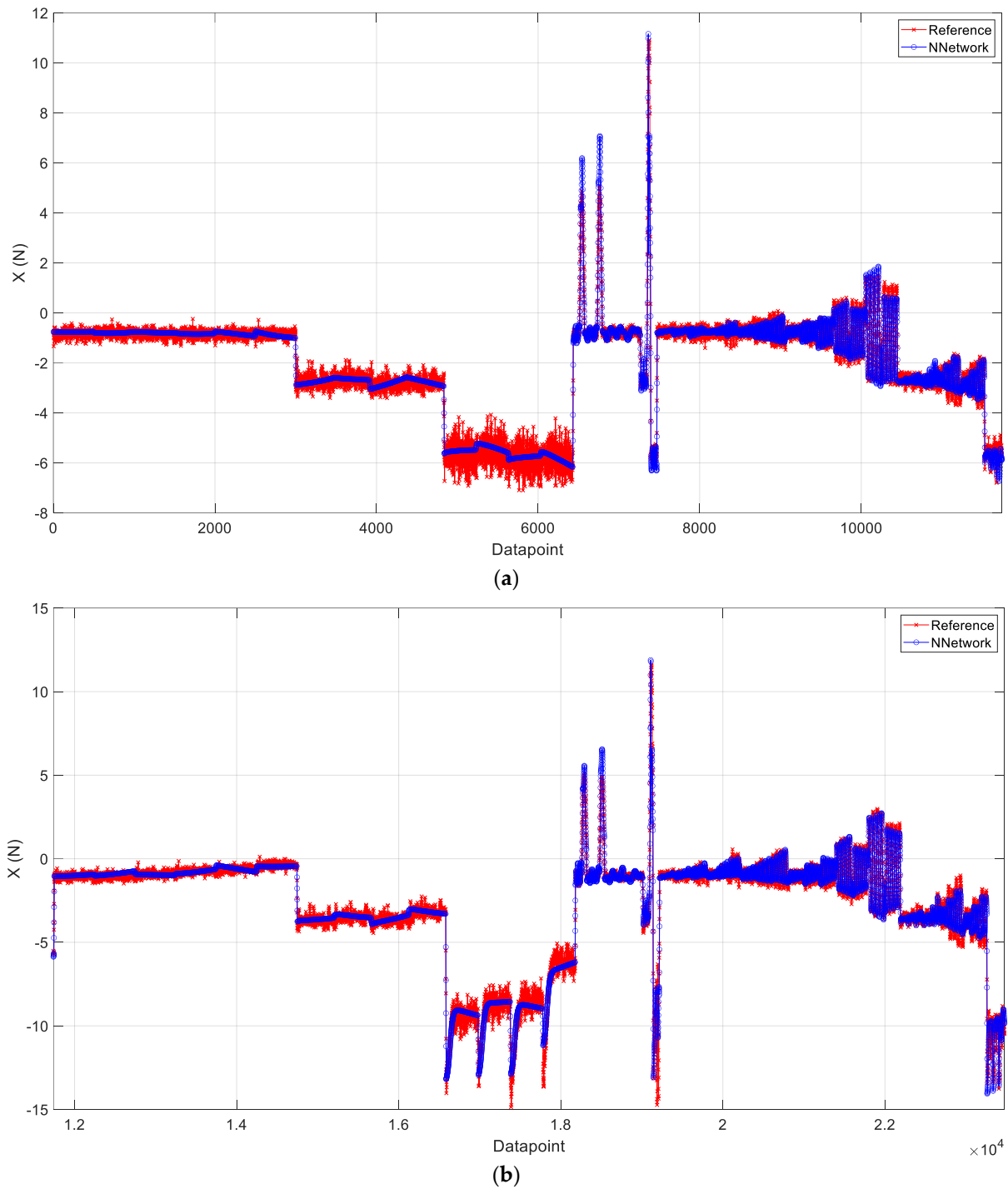
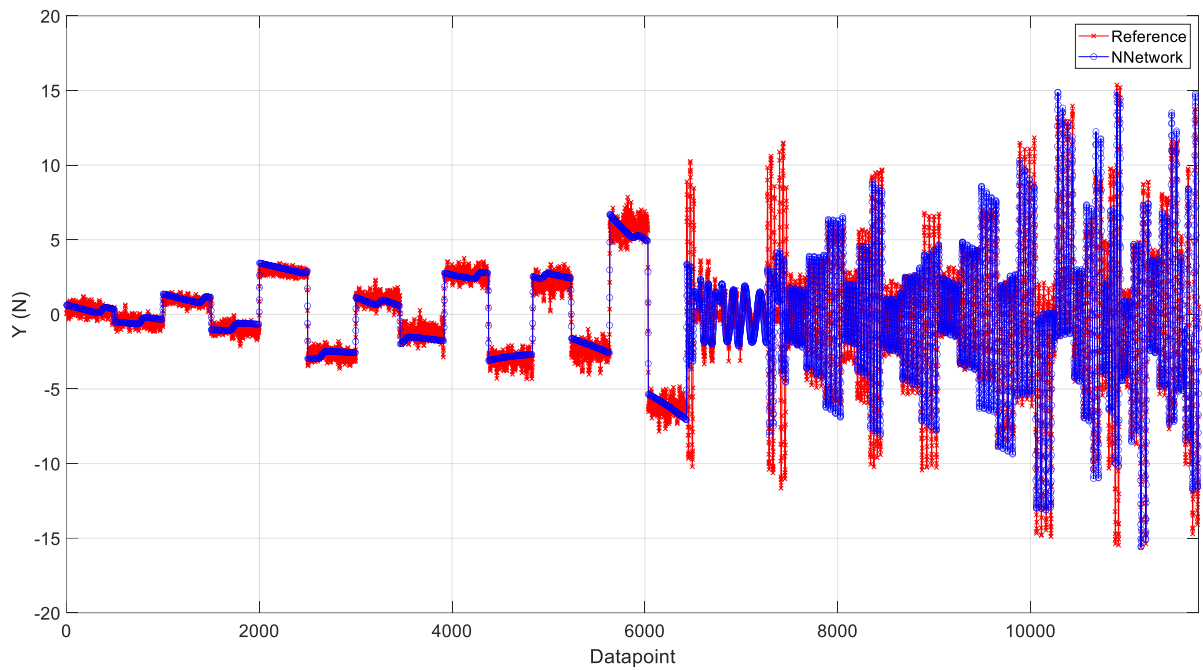


Figure 5. Training results for surge force X prediction in different water depths: (a) $h = 0.3254$ m; (b) $h = 0.1952$ m.

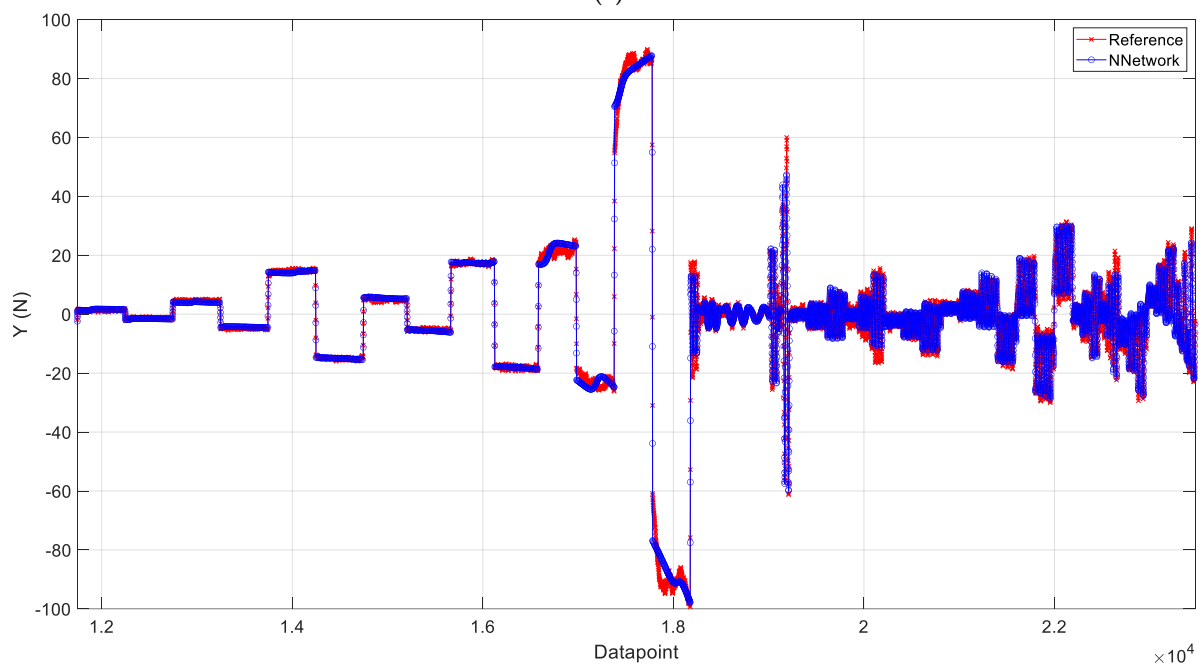
The correlation coefficient r is computed to confirm how much the model output matches the target. As a matter of course, the correlation coefficient among a network output x and a desired output d is stated by the following:

$$r = \frac{\frac{\sum_i (x_i - \bar{x})(d_i - \bar{d})}{N}}{\sqrt{\frac{\sum_i (d_i - \bar{d})^2}{N}} \sqrt{\frac{\sum_i (x_i - \bar{x})^2}{N}}} \tag{12}$$

The r is used to measure the fitness of the obtained results with the ANN model, given in Table 5.



(a)



(b)

Figure 6. Training results for sway force Y prediction in different water depths: (a) $h = 0.3254$ m; (b) $h = 0.1952$ m.

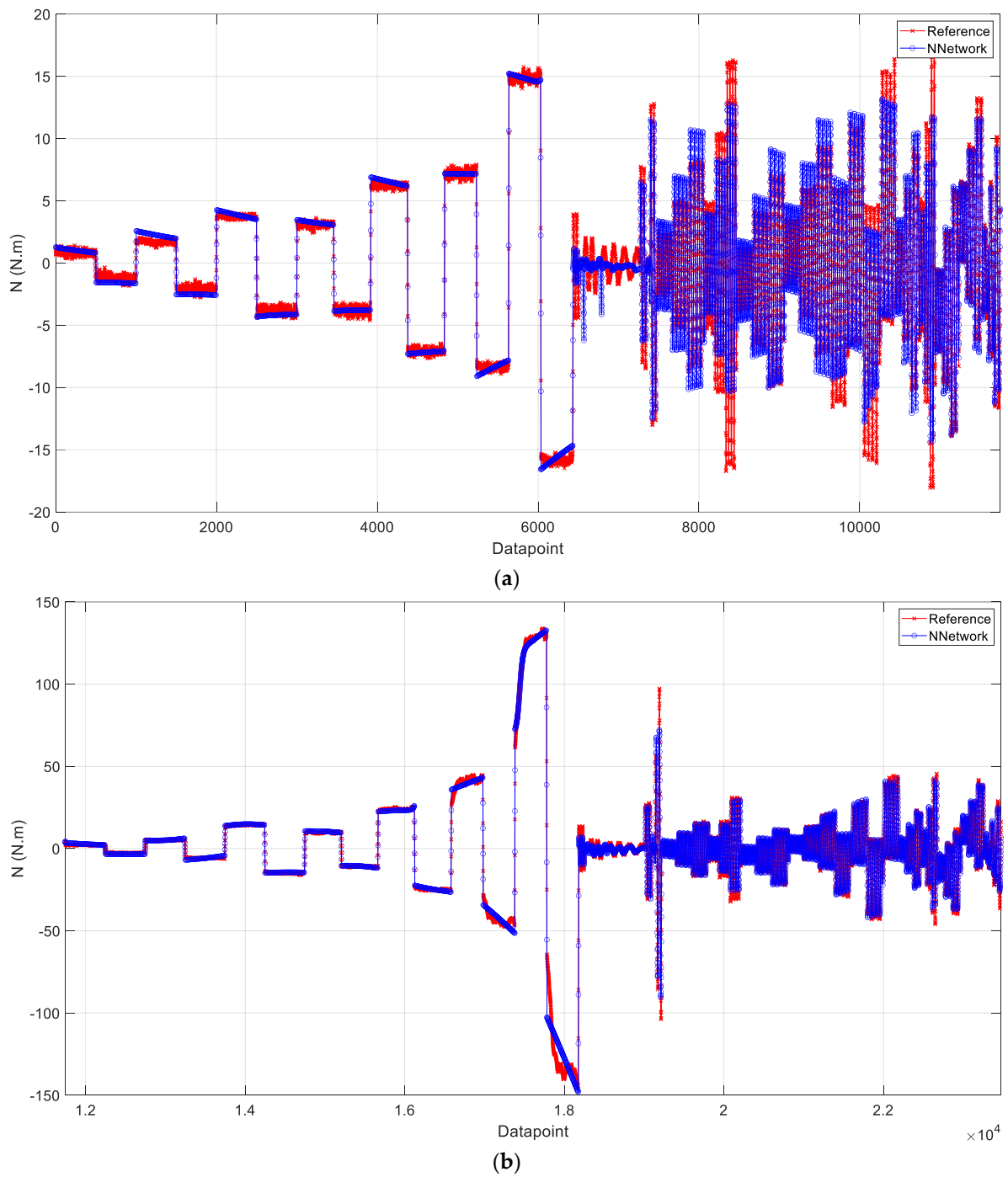


Figure 7. Training results for yaw moment N prediction in different water depths: (a) $h = 0.3254$ m; (b) $h = 0.1952$ m.

From the results presented in Table 5, especially from the observation of the results obtained for the test set, it can be said that the developed design possesses a great generalisation performance, and it can successfully simulate the PMM tests in distinct shallow depths. The results obtained with the ANN models fit the data well in the training, validation, and test sets, using both topologies considered (one hidden layer and three hidden layers). The test set errors are especially important because this set is not employed throughout the training procedure, and it is just utilised to measure the differences between distinct models. In the other hand, the differences obtained using the Levenberg–Marquardt and

resilient backpropagation approaches are minimal, but the Levenberg generally shows slightly better results.

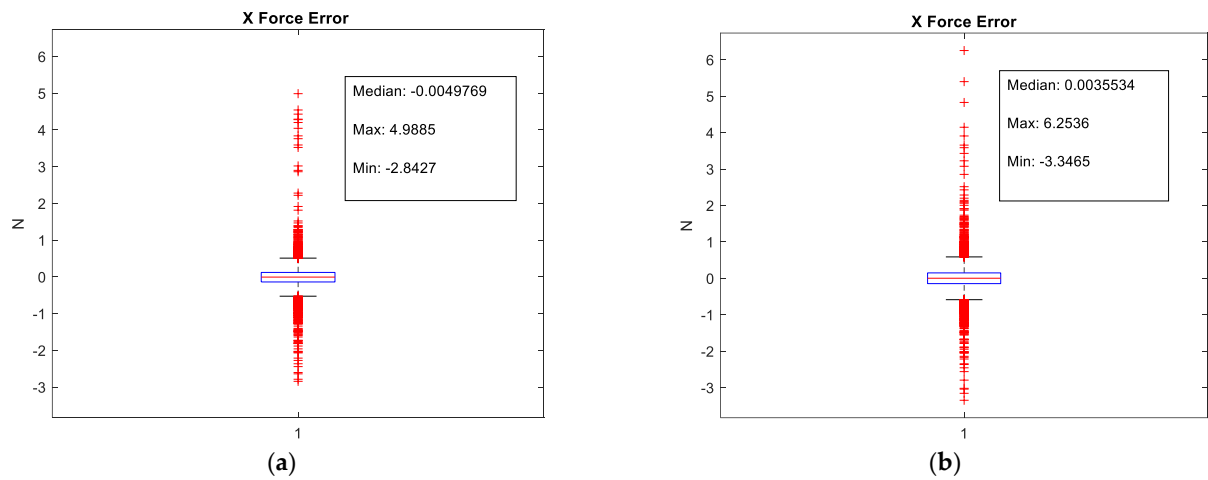


Figure 8. Boxplots of the errors for surge force X prediction in different water depths: (a) $h = 0.3254$ m; (b) $h = 0.1952$ m.

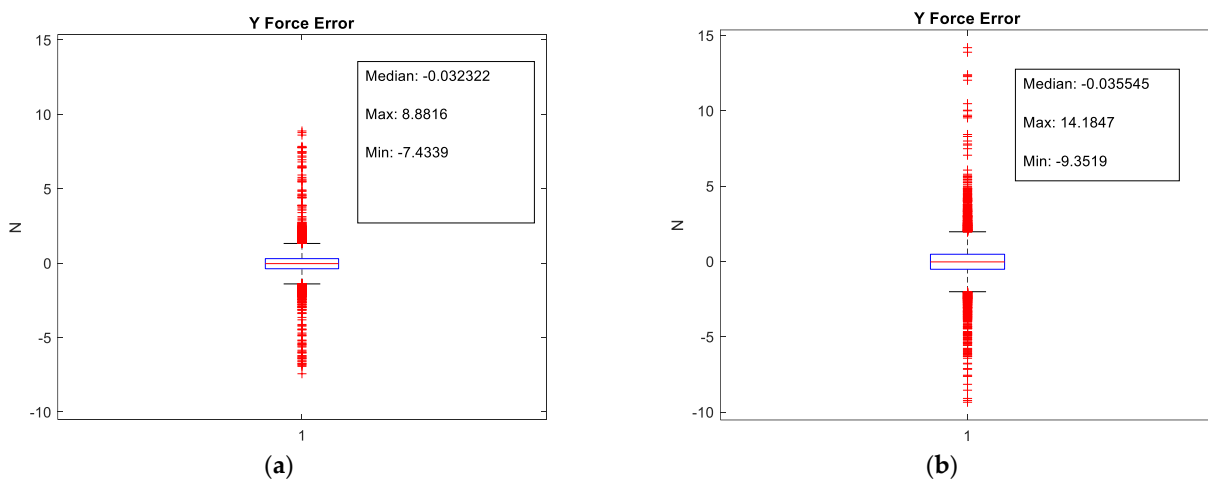


Figure 9. Boxplots of the errors for sway force Y prediction in different water depths: (a) $h = 0.3254$ m; (b) $h = 0.1952$ m.

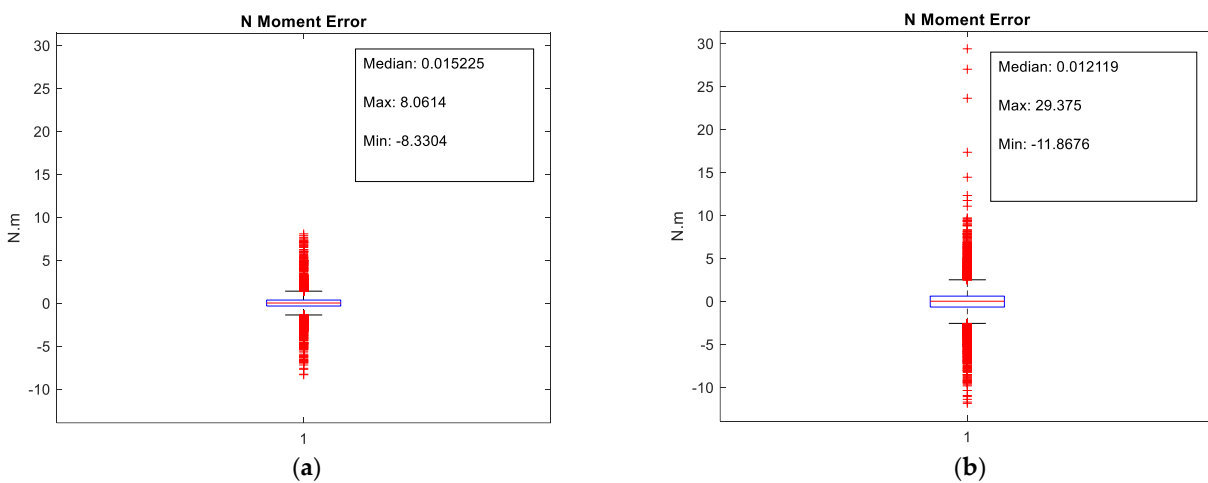


Figure 10. Boxplots of the errors for yaw moment N prediction in different water depths: (a) $h = 0.3254$ m; (b) $h = 0.1952$ m.

Table 5. X, Y, and N error measures (*r*).

Output	# Hidden Layers	# Neurons	Method	Training	Test	Validation
X	1	10	Levenberg	0.98596	0.98664	0.98847
			Resilient B	0.97861	0.97284	0.97922
Y			Levenberg	0.99305	0.99528	0.99346
			Resilient B	0.99122	0.9884	0.99001
N			Levenberg	0.99408	0.99618	0.99215
			Resilient B	0.99578	0.99714	0.99599
X	3	(10, 8, 5)	Levenberg	0.99467	0.99237	0.99276
			Resilient B	0.99087	0.98813	0.98877
Y			Levenberg	0.99707	0.99647	0.99567
			Resilient B	0.99649	0.99614	0.99617
N			Levenberg	0.99811	0.99783	0.99855
			Resilient B	0.99797	0.99807	0.99827

Figures 11–13 present the surge speed, sway speed, and yaw rate assessed in the free-running tests in shallow water and the related estimations obtained through the ANN model using the resilient backpropagation method with three hidden layers in the network structure. Figures 14–16 present boxplots of the errors obtained in the predictions shown in Figures 11–13, respectively.

According to Figures 11–13, the ANN model can reproduce surge and sway velocities and a yaw rate in excellent agreement with the measured results obtained in the PMM tests. From the boxplot of Figure 14, which compares the central tendencies of the surge velocity *u* for the two different depths, it can be verified that the median is slightly similar. The variability for both depths does not exhibit relevant discrepancy, and it can be perceived that the distribution of the obtained error is left-skewed. Similar results are obtained for the boxplot of the sway velocity *v* presented in Figure 15, but a symmetrical distribution is noticed in this case. For the boxplot of the yaw rate *r* shown in Figure 16, there are also approximately symmetrical distributions for the errors.

The *r* values of the estimations are provided in Table 6.

Table 6. Surge, sway, and yaw velocity error measurements (*r*).

Output	# Hidden Layers	# Neurons	Method	Training	Test	Validation
<i>u</i>	1	10	Levenberg	0.99271	0.99128	0.99318
			Resilient B	0.99175	0.99089	0.99086
<i>v</i>			Levenberg	0.96641	0.96233	0.96671
			Resilient B	0.97282	0.97523	0.97374
<i>r</i>			Levenberg	0.96527	0.96369	0.96671
			Resilient B	0.96428	0.96278	0.96497
<i>u</i>	3	(10, 8, 5)	Levenberg	0.99792	0.99418	0.99634
			Resilient B	0.99899	0.99553	0.99882
<i>v</i>			Levenberg	0.98281	0.98202	0.98263
			Resilient B	0.98369	0.98091	0.98329
<i>r</i>			Levenberg	0.98799	0.98543	0.98584
			Resilient B	0.98549	0.9855	0.98465

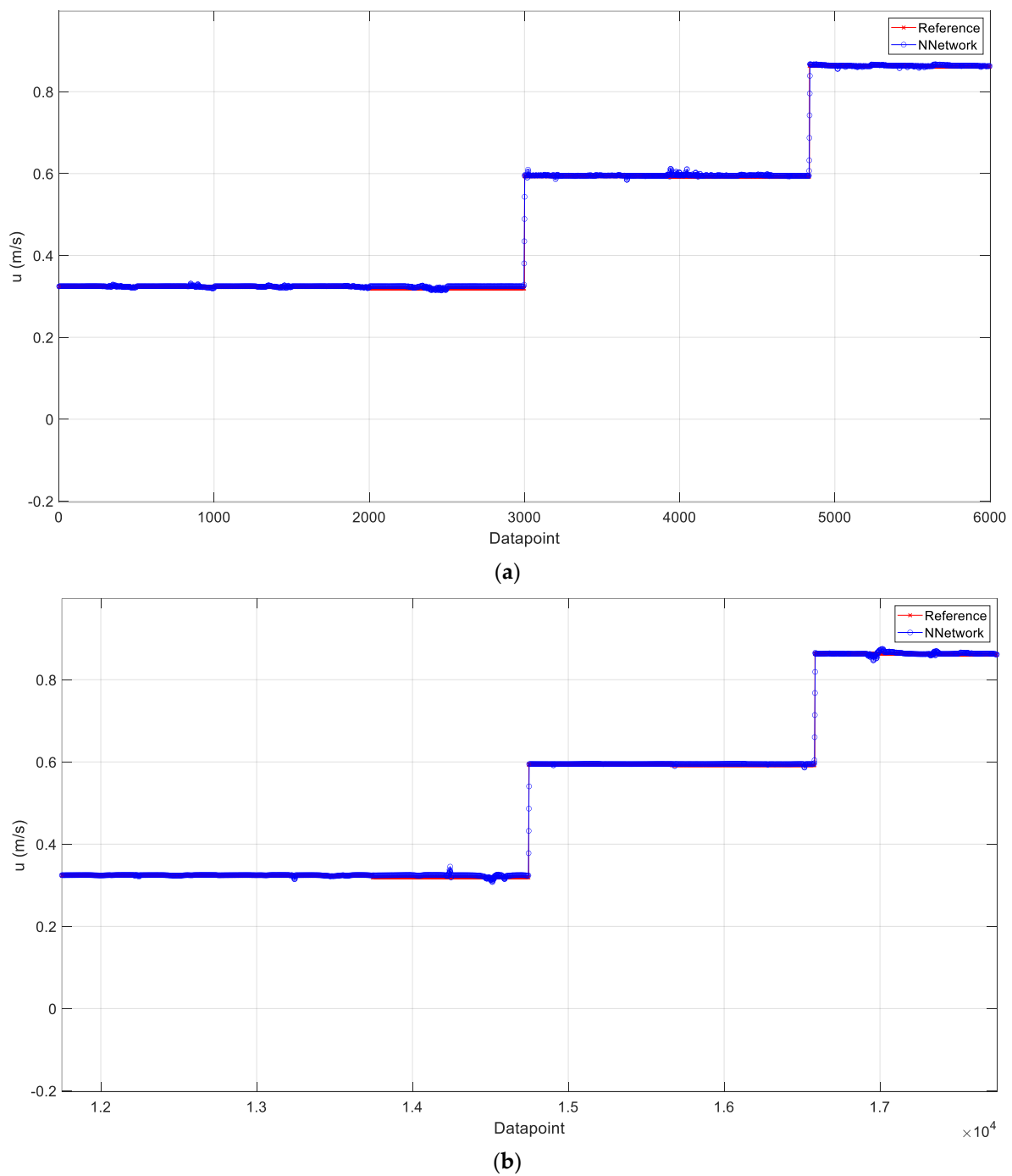
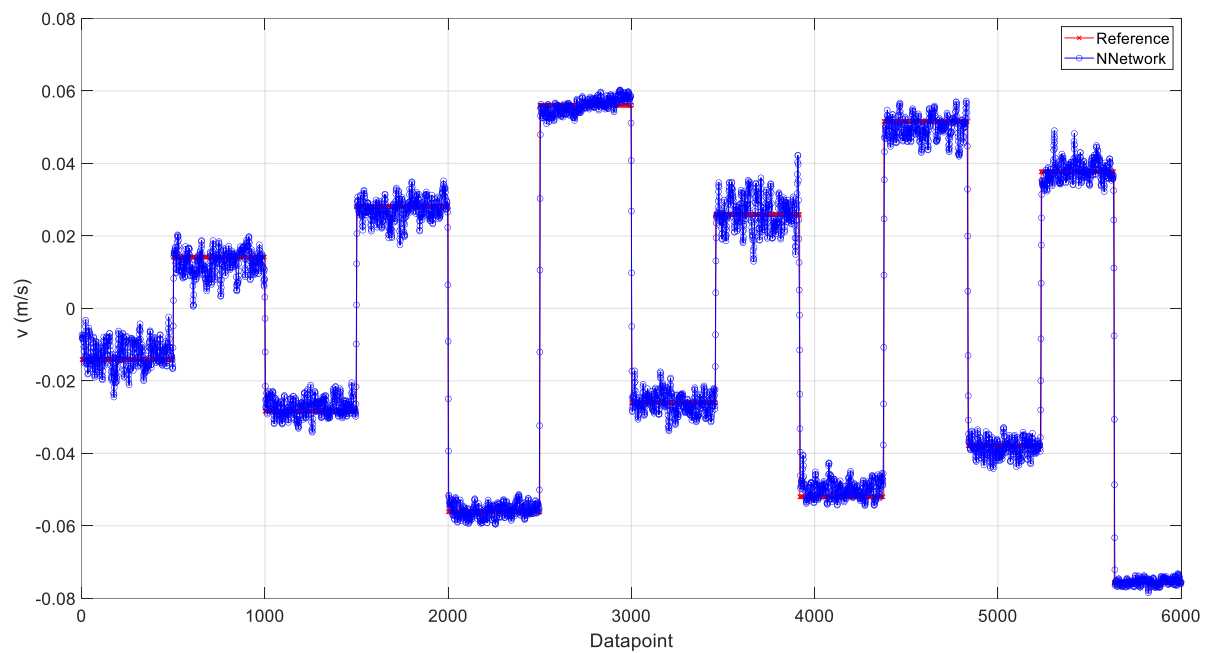


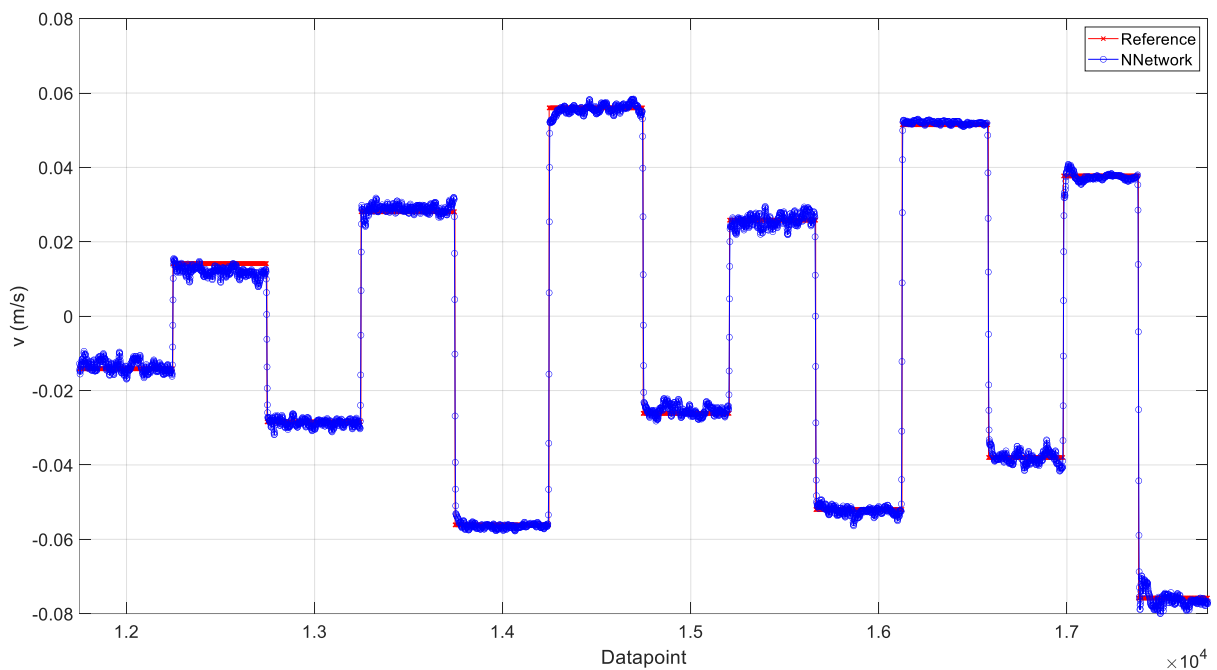
Figure 11. Training results for surge velocity u prediction in different water depths: (a) $h = 0.3254$ m; (b) $h = 0.1952$ m.

Table 6 demonstrates that the derived system has an excellent generalisation performance and can reproduce the dynamic characteristics of the free-running model tests at shallow depths. From the results presented in Table 6, in a similar way as concluded from Table 5, it can be said that the developed system exhibits very good generalisation performance and can successfully simulate the PMM model tests in diverse water depths. The results obtained with the ANN models fit the data in the training, validation, and test sets very well, using both topologies (one hidden layer and three hidden layers). As previously explained for the results obtained in Table 5, the observation of the results obtained for the test set are especially important drawing conclusions about the model's

generalisation performance and its capability to successfully simulate the PMM tests in distinct shallow depths.



(a)



(b)

Figure 12. Training results for sway velocity v prediction in different water depths: (a) $h = 0.3254$ m; (b) $h = 0.1952$ m.

In the case of the surge and sway velocities and yaw rate estimations, the differences between the results obtained using the Levenberg–Marquardt and resilient backpropagation approaches are again very small. In Tables 5 and 6, the results for three hidden layers represent a sensitivity check on the capabilities of one hidden layer to provide appropriate results.

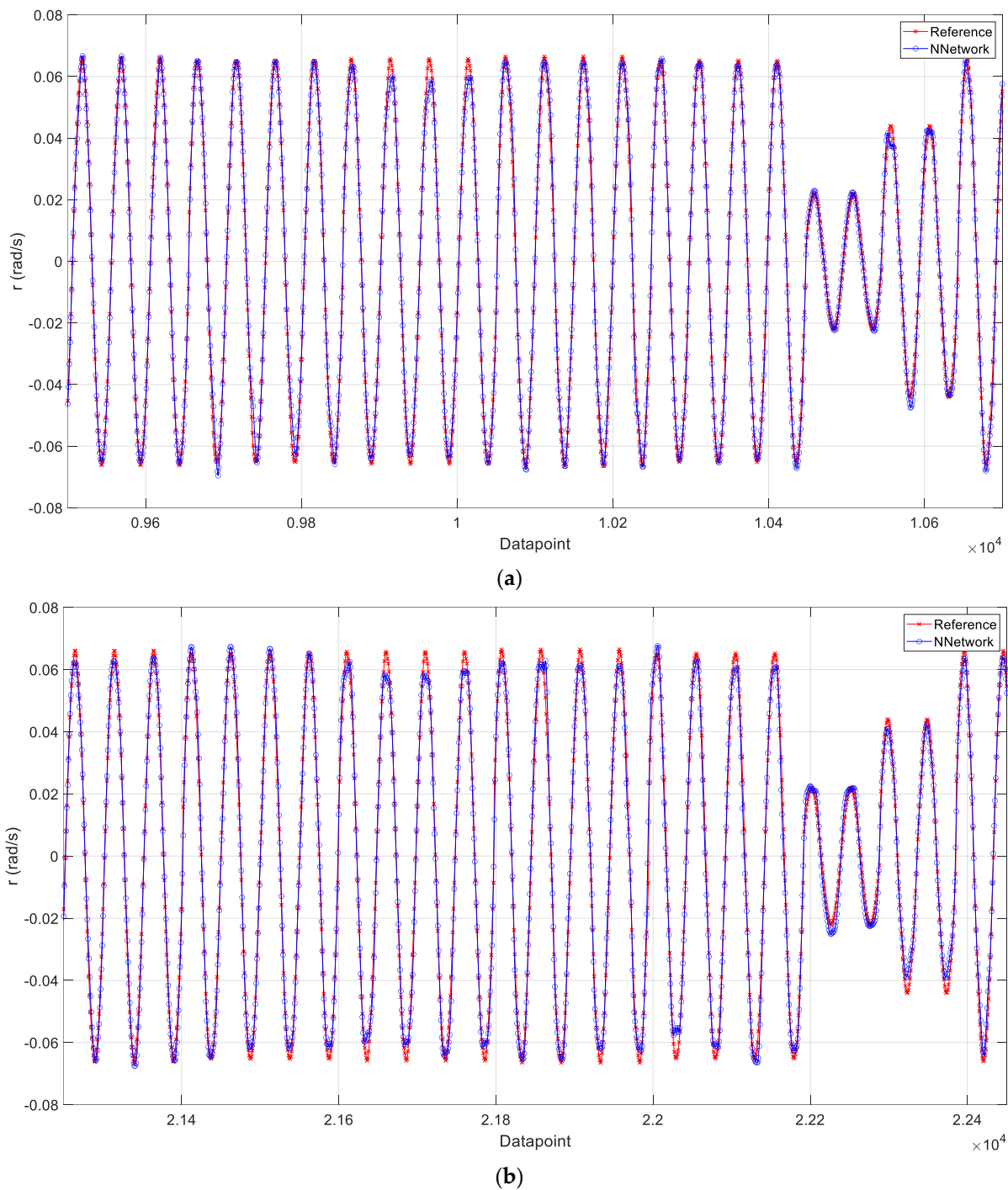


Figure 13. Training results for yaw rate r prediction in different water depths: (a) $h = 0.3254$ m (b) $h = 0.1952$ m.

As final considerations for this study, an NN model suitable for performing ship manoeuvrability predictions in different shallow water conditions was proposed and implemented. The motivation and advantages behind the development of this type of novel model were well justified. There are no evident differences in the results obtained using either the Levenberg–Marquardt algorithm or the resilient backpropagation procedure. As expected, slightly better results were achieved using three hidden layers than just one hidden layer in the NN structure. From the values achieved of the error r , from the figures of the superposition of the predicted values with the experimental data, and from the boxplots of the errors, it is evident that the proposed ANN model has very good performance and

that it is a valid model for estimating manoeuvring characteristics of ships under different shallow-water conditions. The effectiveness of the good generalisation capability of the proposed model was confirmed by the very good values of r achieved in the test set.

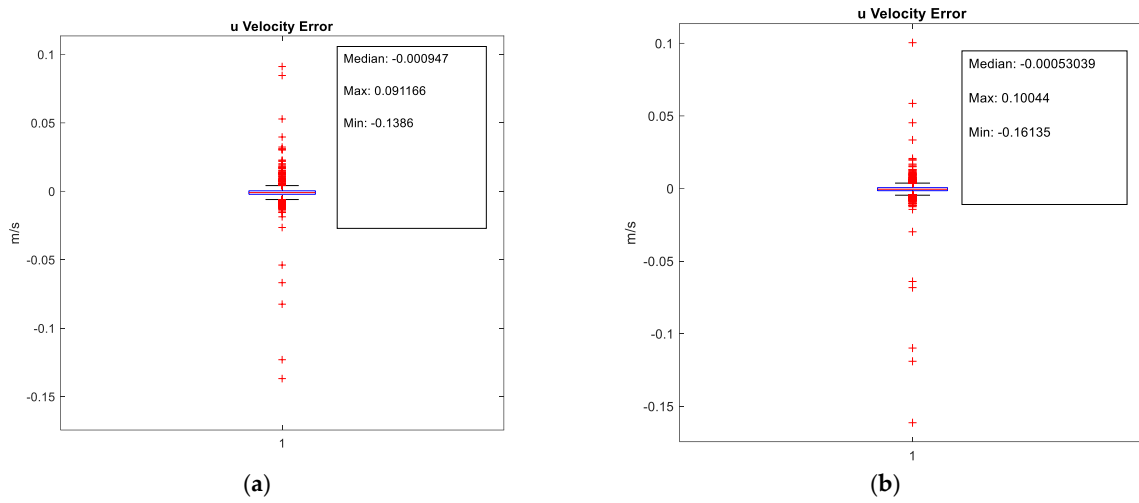


Figure 14. Boxplots of the error for surge velocity u prediction in different water depths: (a) $h = 0.3254$ m; (b) $h = 0.1952$ m.

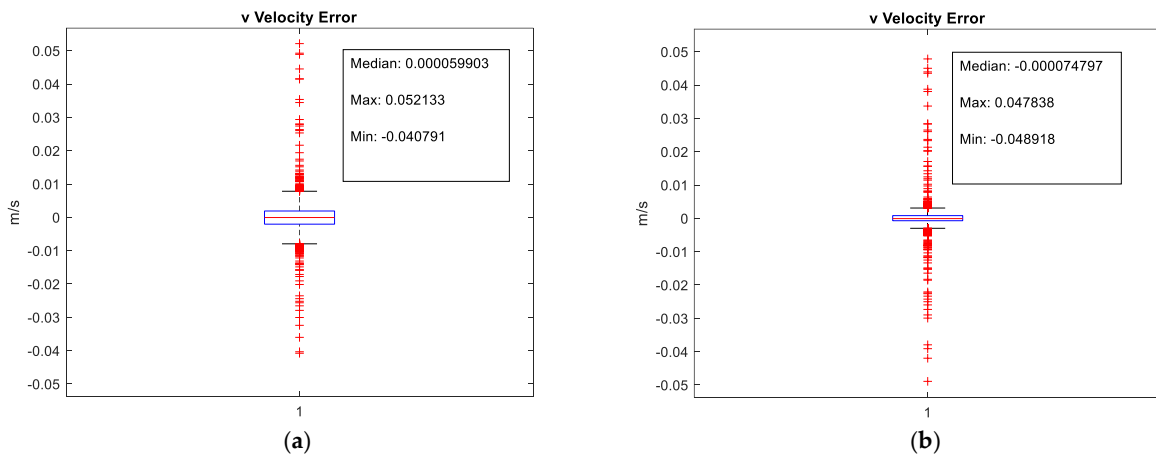


Figure 15. Boxplots of the error for sway velocity v prediction in different water depths: (a) $h = 0.3254$ m; (b) $h = 0.1952$ m.

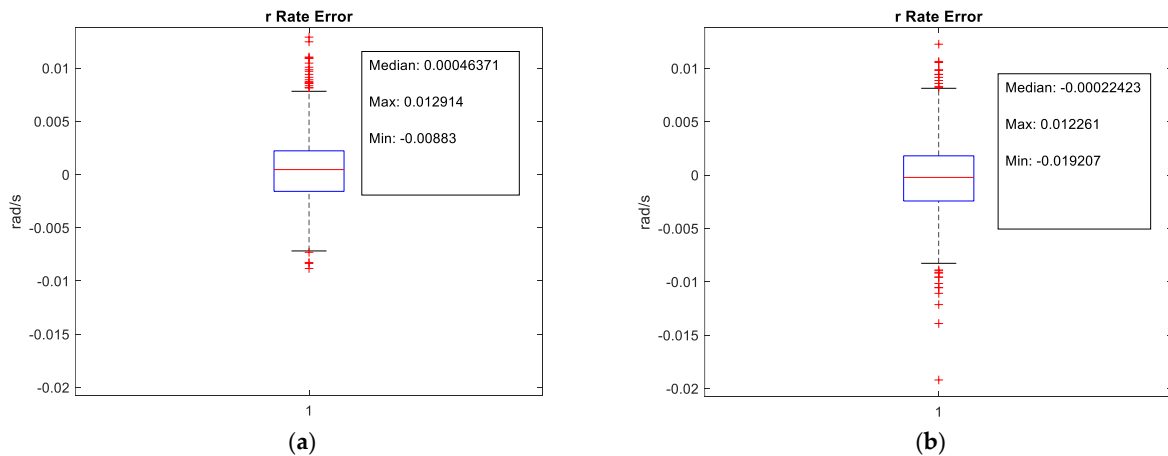


Figure 16. Boxplots of the error for yaw rate r prediction in different water depths: (a) $h = 0.3254$ m; (b) $h = 0.1952$ m.

5. Conclusions

The current work has shown the validity of the NNs model as a predictor of the manoeuvring behaviour of a Post-Panamax container ship model in shallow water with data obtained in a series of PMM tests. The past research devoted to NN applications of ship manoeuvrability in shallow depths is insufficient for drawing conclusions about their capability to learn the respective effects, and this article intends to contribute by analysing an ANN system's capabilities to predict the vessel's manoeuvring qualities in distinct shallow depths. This topic is of great importance due to the continuing trend towards ever-larger vessels and their use in shallow waters. The ANN model for vessel manoeuvrability prediction in shallow depths has been designed using two different methods for comparison: the Levenberg–Marquardt backpropagation and the resilient backpropagation. An explanation for the choice of apparatus used for the experimental tests that provided the data used for the NN training was given in Section 2. The designed model can predict the motions measured in the PMM tests performed with the model in shallow water and has demonstrated a good degree of precision in estimating the vessel manoeuvring performance in different depths. The generalisation performance of the developed ANN systems was examined through the test and validation sets. The obtained correlation coefficient r results have demonstrated that the developed ANN models have excellent generalisation performance and may be employed to reproduce the vessel dynamics when manoeuvring in shallow depths. The analysis presented in this paper has only examined the manoeuvring characteristics of the vessel model in two shallow depths. Even though the outcomes presented in this paper are for a given benchmarking vessel model, the results might apply to any real-scale ship if the appropriate training data are available. In the case of real scenarios, external disturbances might be included as inputs, especially wind and current for this specific application. The ANN model is a viable alternative for onboard ship simulators and decision support systems.

Author Contributions: Funding acquisition, C.G.S.; formal analysis, L.M.; writing—original draft, L.M.; writing—review and editing, C.G.S.; methodology, L.M.; software, L.M.; supervision, C.G.S. All authors have read and agreed to the published version of the manuscript.

Funding: This work was performed within the scope of the Strategic Research Plan of the Centre for Marine Technology and Ocean Engineering (CENTEC), which is financed by the Portuguese Foundation for Science and Technology (Fundação para a Ciência e Tecnologia—FCT) under contract UIDB/UIDP/00134/2020.

Institutional Review Board Statement: Not applicable.

Informed Consent Statement: Not applicable.

Data Availability Statement: The original contributions presented in the study are included in the article, further inquiries can be directed to the corresponding author.

Conflicts of Interest: The authors declare no conflicts of interest.

Abbreviations

AI	Artificial intelligence
ANN	Artificial neural network
AT-NN	Attention-based neural network
BEM	Boundary element method
Bi-LSTM	Bidirectional long short-term memory
CFD	Computational fluid dynamics
CNN	Convolutional neural network
COG	Course over ground
Conv-1D	One-dimensional convolution
DMD	Dynamic mode decomposition
DTC	Duisburg Test Case

DTMB	David Taylor Model Basin
FHR	Flanders Hydraulics Research
GPR	Gaussian process regression
GRU	Gated recurrent units
IADPSO	Improved adaptive particle swarm optimisation
IMO	International Maritime Organization
ITTC	International Towing Tank Conference
KCS	KRISO container ship
LMS	Least mean squares
LS-SVM	Least-squares support vector machine
LSTM	Long short-term memory
MAE	Mean absolute error
MLP	Multilayer perceptron
MMG	Mathematical manoeuvring group
MRNN	Multi-recurrent neural network
MSE	Mean squared error
NN	Neural network
NSE	Nash–Sutcliffe efficiency
PE	Processing element
PMM	Planar motion mechanism
QEA	Quantum-inspired evolutionary algorithm
RANS	Reynolds-averaged Navier–Stokes
RNN	Recurrent neural network
RPM	Revolutions per minute
SAWB	Ship as a wave buoy
SDN-HP	Self-organising data-driven network with hierarchical pruning
SSE	Sea state estimation
SVR	Support vector regression
TEU	Twenty-foot equivalent unit

References

1. Taimuri, G.H.; Matusiak, J.; Mikkola, T.; Kujala, P.; Hirdaris, S.E. A 6-DoF maneuvering model for the rapid estimation of hydrodynamic actions in deep and shallow waters. *Ocean Eng.* **2020**, *218*, 108103. [[CrossRef](#)]
2. IMO. *Explanatory Notes to the Standards for Ship Manoeuvrability*; International Maritime Organization: London, UK, 2002.
3. ITTC. The Specialist Committee on Esso Osaka—Final Report and Recommendations to the 23rd ITTC. In Proceedings of the International Towing Tank Conference 2002, Venice, Italy, 8–14 September 2002.
4. SHOPERA (2013–2016). Available online: <https://cordis.europa.eu/project/id/605221/reporting> (accessed on 26 October 2023).
5. Shigunov, V.; Papanikolaou, A. Criteria for minimum powering and manoeuvrability in adverse weather conditions. In Proceedings of the 14th International Ship Stability Workshop ISSW, Kuala Lumpur, Malaysia, 29 September–1 October 2014.
6. Papanikolaou, A.; Zaraphonitis, G.; Bitner-Gregersen, E.; Shigunov, V.; Moctar, O.E.; Soares, C.G.; Reddy, D.N.; Sprenger, F. Energy efficient Safe Ship operation (SHOPERA). *Transp. Res. Procedia* **2016**, *14*, 820–829. [[CrossRef](#)]
7. Van Zwijnsvoorde, T.; Tello Ruiz, M.; Delefortrie, G.; Lataire, E. Sailing in Shallow Water Waves with the DTC Container Carrier: Open Model Test Data for Validation Purposes. In Proceedings of the 5th International Conference on Ship Manoeuvring in Shallow and Confined Water (MASHCON), Ostend, Belgium, 20–22 May 2019; Volume 5.
8. Cura-Hochbaum, A.; Uharek, S. Prediction of the manoeuvring behaviour of the KCS based on virtual captive tests. In Proceedings of the Workshop on Verification and Validation of Ship Manoeuvring Simulation Methods (SIMMAN), Lyngby, Denmark, 8–10 December 2014.
9. Xu, H.; Hassani, V.; Guedes Soares, C. Uncertainty analysis of the hydrodynamic coefficients estimation of a non-linear manoeuvring model based on planar motion mechanism tests. *Ocean Eng.* **2019**, *173*, 450–459. [[CrossRef](#)]
10. Xu, H.; Hassani, V.; Guedes Soares, C. Truncated least square support vector machine for parameter estimation of a non-linear manoeuvring model based on PMM tests. *Appl. Ocean Res.* **2020**, *97*, 102076. [[CrossRef](#)]
11. Islam, H.; Guedes Soares, C. Estimation of hydrodynamic derivatives of an appended KCS model in open and restricted waters. *Ocean Eng.* **2022**, *266*, 112947. [[CrossRef](#)]
12. Yoshimura, Y. Mathematical model for the manoeuvring ship motion in shallow water. *J. Jpn. Soc. Nav. Archit. Ocean. Eng. (KASNAJ)* **1986**, *200*, 41–51.
13. Tezdogan, T.; Incecik, A.; Turan, O. Full-scale unsteady RANS simulations of vertical ship motions in shallow water. *Ocean Eng.* **2016**, *123*, 131–145. [[CrossRef](#)]

14. Liu, J.; Hekkenberg, R.; Rotteveel, E. A proposal for standard manoeuvres and parameters for the evaluation of inland ship manoeuvrability. In Proceedings of the European Inland Waterway Navigation Conference, Budapest, Hungary, 10–12 September 2014. [[CrossRef](#)]
15. Kim, D.; Tezdogan, T.; Incecik, A. Hydrodynamic analysis of ship manoeuvrability in shallow water using high-fidelity URANS computations. *Appl. Ocean Res.* **2022**, *123*, 103176. [[CrossRef](#)]
16. Martić, I.; Degiuli, N.; Borčić, K.; Grlj, C. Numerical Assessment of the Resistance of a Solar Catamaran in Shallow Water. *J. Mar. Sci. Eng.* **2023**, *11*, 1706. [[CrossRef](#)]
17. Hadi, E.; Tuswan, T.; Azizah, G.; Ali, B.; Samuel, S.; Hakim, M.; Hadi, M.; Iqbal, M.; Sari, D.; Satrio, D. Influence of the canal width and depth on the resistance of 750 DWT Perintis ship using CFD simulation. *Brodogradnja* **2023**, *74*, 117–144. [[CrossRef](#)]
18. Moreira, L.; Guedes Soares, C. Dynamic model of manoeuvrability using recursive neural networks. *Ocean Eng.* **2003**, *30*, 1669–1697. [[CrossRef](#)]
19. Lacki, M. Intelligent Prediction of Ship Maneuvering. *TransNav Int. J. Mar. Navig. Saf. Sea Transp.* **2016**, *10*, 511–516. [[CrossRef](#)]
20. Moreira, L.; Guedes Soares, C. Simulating Ship Manoeuvrability-with Artificial Neural Networks Trained by a Short Noisy Data Set. *J. Mar. Sci. Eng.* **2022**, *11*, 15. [[CrossRef](#)]
21. Chen, X.; Meng, X.; Zhao, Y. Genetic algorithm to improve Back Propagation Neural Network ship track prediction. *J. Phys. Conf. Ser.* **2020**, *1650*, 032133. [[CrossRef](#)]
22. Ahmed, Y.A.; Kamal, I.Z.M.; Hannan, M.A. An artificial neural network controller for course changing manoeuvring. *Int. J. Innov. Technol. Explor. Eng.* **2019**, *8*, 5714–5719. [[CrossRef](#)]
23. Ahmed, Y.A.; Hannan, M.A.; Kamal, I.M. Minimum time ship manoeuvring in narrow water ways under wind disturbances. In Proceedings of the ASME 37th International Conference on Ocean, Offshore and Arctic Engineering 2018, Madrid, Spain, 17–22 June 2018. OMAE2018-78435.
24. Araújo, J.P.; Moreira, L.; Guedes Soares, C. Modelling ship manoeuvrability using recurrent neural networks. In *Developments in Maritime Technology and Engineering*; Guedes Soares, C., Santos, T.A., Eds.; Taylor and Francis: London, UK, 2021; Volume 2, pp. 131–140.
25. Luo, W.; Zhang, Z. Modeling of ship maneuvering motion using neural networks. *J. Mar. Sci. Appl.* **2016**, *15*, 426–432. [[CrossRef](#)]
26. Dong, Q.; Wang, N.; Song, J.; Lizhu, H.; Liu, S.; Han, B.; Qu, K. Math-data integrated prediction model for ship maneuvering motion. *Ocean Eng.* **2023**, *285*, 115255. [[CrossRef](#)]
27. International Maritime Organization. *Interim Guidelines for Determining Minimum Propulsion Power to Maintain the Manoeuvrability of Ships in Adverse Conditions, IMO Resolution MEPC*; International Maritime Organization: London, UK, 2013; Volume 232.
28. Martić, I.; Degiuli, N.; Majetic, D.; Farkas, A. Artificial Neural Network Model for the Evaluation of Added Resistance of Container Ships in Head Waves. *J. Mar. Sci. Eng.* **2021**, *9*, 826. [[CrossRef](#)]
29. Martić, I.; Degiuli, N.; Grlj, C. Prediction of Added Resistance of Container Ships in Regular Head Waves Using an Artificial Neural Network. *J. Mar. Sci. Eng.* **2023**, *11*, 1293. [[CrossRef](#)]
30. D’Agostino, D.; Serani, A.; Stern, F.; Diez, M. Time-series forecasting for ships maneuvering in waves via recurrent-type neural networks. *J. Ocean Eng. Mar. Energy* **2022**, *8*, 479–487. [[CrossRef](#)]
31. Wang, N.; Kong, X.; Ren, B.; Hao, L.; Han, B. SeaBil: Self-attention-weighted ultrashort-term deep learning prediction of ship maneuvering motion. *Ocean Eng.* **2023**, *287*, 115890. [[CrossRef](#)]
32. Wang, N.; Wu, H.; Zhang, Y.; Song, J.; Lin, Y.; Hao, L. Self-organizing data-driven prediction model of ship maneuvering fast-dynamics. *Ocean Eng.* **2023**, *288*, 115989. [[CrossRef](#)]
33. Silva, K.; Maki, K. Data-Driven system identification of 6-DoF ship motion in waves with neural networks. *Appl. Ocean Res.* **2022**, *125*, 103222. [[CrossRef](#)]
34. Sun, Q.; Tang, Z.; Gao, J.; Zhang, G. Short-term ship motion attitude prediction based on LSTM and GPR. *Appl. Ocean Res.* **2022**, *118*, 102927. [[CrossRef](#)]
35. Long, N.; Sgarioto, D.; Garratt, M.; Sammut, K. Response component analysis for sea state estimation using artificial neural networks and vessel response spectral data. *Appl. Ocean Res.* **2022**, *127*, 103320. [[CrossRef](#)]
36. Romero-Tello, P.; Gutierrez-Romero, J.E.; Servan-Camas, B. Prediction of seakeeping in the early stage of conventional monohull vessels design using Artificial Neural Network. *J. Ocean Eng. Sci.* **2022**. [[CrossRef](#)]
37. Selimović, D.; Hrzic, F.; Prpic-Orsic, J.; Lerga, J. Estimation of sea state parameters from ship motion responses using attention-based neural networks. *Ocean Eng.* **2023**, *281*, 114915. [[CrossRef](#)]
38. Zhang, L.; Feng, X.; Wang, L.; Gong, B.; Ai, J. A hybrid ship-motion prediction model based on CNN-MRNN and IADPSO. *Ocean Eng.* **2024**, *299*, 117428. [[CrossRef](#)]
39. Wakita, K.; Maki, A.; Umeda, N.; Miyauchi, Y.; Shimoji, T.; Rachman, D.; Akimoto, Y. On neural network identification for low-speed ship maneuvering model. *J. Mar. Sci. Technol.* **2022**, *27*, 772–785. [[CrossRef](#)]
40. Sano, M. Mathematical model and simulation of cooperative manoeuvres among a ship and tugboats. *Brodogradnja* **2023**, *74*, 127–148. [[CrossRef](#)]
41. Xu, H.; Guedes Soares, C. Hydrodynamic coefficient estimation for ship manoeuvring in shallow water using an optimal truncated LS-SVM. *Ocean Eng.* **2019**, *191*, 106488. [[CrossRef](#)]

42. Xu, H.; Guedes Soares, C. Manoeuvring modelling of a containership in shallow water based on optimal truncated non-linear kernel-based least square support vector machine and quantum-inspired evolutionary algorithm. *Ocean Eng.* **2020**, *195*, 106676. [[CrossRef](#)]
43. Moctar, O.; El Shigunov, V.; Zorn, T. Duisburg test case: Post-panamax container ship for benchmarking. *Ship Technol. Res.* **2012**, *59*, 50–64. [[CrossRef](#)]
44. Moreira, L.; Guedes Soares, C. Analysis of recursive neural networks performance trained with noisy manoeuvring data. In *Maritime Transportation and Exploitation of Ocean and Coastal Resources*; Guedes Soares, C., Garbatov, Y., Fonseca, N., Eds.; Taylor & Francis Group: Oxfordshire, UK, 2005; pp. 733–744.
45. Moreira, L.; Guedes Soares, C. Recursive neural network model of catamaran manoeuvring. *Int. J. Marit. Eng.* **2012**, *154*, A3. [[CrossRef](#)]
46. Delefortrie, G.; Vantorre, M. Experimental studies on seakeeping and maneuverability of ships in adverse weather conditions. *J. Ship Res.* **2007**, *51*, 287–296. [[CrossRef](#)]
47. Eloot, K.; Vantorre, M.; Delefortrie, G.; Lataire, E. Running sinkage and trim of the DTC container carrier in harmonic sway and yaw motion: Open model test data for validation purposes. In *Proceedings of the 4th International Conference on Ship Manoeuvring in Shallow and Confined Water (MASHCON): Ship Bottom Interaction*, Hamburg, Germany, 23–25 May 2016; Uliczka, K., Bottner, C.-U., Kastens, M., Eloot, K., Delefortrie, G., Vantorre, M., Candries, M., Lataire, E., Eds.; Bundesanstalt für Wasserbau: Hamburg, Germany, 2016; pp. 251–261.
48. Eloot, K.; Vantorre, M. Alternative Captive Manoeuvring Tests: Possibilities and Limitations. In *Proceedings of the International Symposium and Workshop on Force Acting on a Manoeuvring Vessel*, Val de Reuil, France, 16–18 September 1998.
49. Delefortrie, G.; Eloot, K.; Lataire, E.; Van Hoydonck, W.; Vantorre, M. Captive model tests based 6 DOF shallow water manoeuvring model. In *Proceedings of the 4th MASHCON-International Conference on Ship Manoeuvring in Shallow and Confined Water with Special Focus on Ship Bottom Interaction*, Hamburg, Germany, 23–25 May 2016; pp. 273–286.
50. Delefortrie, G.; Geerts, S.; Vantorre, M. The towing tank for manoeuvres in shallow water. In *Proceedings of the 4th MASHCON-International Conference on Ship Manoeuvring in Shallow and Confined Water with Special Focus on Ship Bottom Interaction*, Hamburg, Germany, 23–25 May 2016; pp. 226–235.
51. Van Kerkhove, G.; Vantorre, M.; Delefortrie, G. Advanced Model Testing Techniques for Ship Behaviour in Shallow and Confined Water. In *Proceedings of the AMT*, Nantes, France, 1–2 September 2009.
52. Lippmann, R.P. An introduction to computing with neural nets. *IEEE Trans. ASSP Mag.* **1987**, *4*, 4–22. [[CrossRef](#)]
53. Makhoul, J. Pattern recognition properties of neural networks. In *Proceedings of the 1991 IEEE Workshop on Neural Networks for Signal Processing*, Princeton, NJ, USA, 29 September–2 October 1991.
54. Riedmiller, M.; Braun, H. A direct adaptive method for faster backpropagation learning: The RPROP algorithm. In *Proceedings of the IEEE International Conference on Neural Networks (ICNN'93)*, San Francisco, CA, USA, 28 March–1 April 1993.
55. Hush, D.R.; Horne, B.G. Progress in supervised neural networks. *IEEE Signal Process. Mag.* **1993**, *10*, 8–39. [[CrossRef](#)]
56. Bishop, C.M. *Pattern Recognition and Machine Learning*; Springer: Berlin/Heidelberg, Germany, 2006.

Disclaimer/Publisher's Note: The statements, opinions and data contained in all publications are solely those of the individual author(s) and contributor(s) and not of MDPI and/or the editor(s). MDPI and/or the editor(s) disclaim responsibility for any injury to people or property resulting from any ideas, methods, instructions or products referred to in the content.